

Telocytes in human skin – are they involved in skin regeneration?

Laura Ceafalan ^{a, b}, Mihaela Gherghiceanu ^c, L. M. Popescu ^{c, *}, Olga Simionescu ^{d, *}

^a Molecular Medicine Laboratory, “V. Babeş” National Institute of Pathology, Bucharest, Romania

^b Department of Cellular and Molecular Medicine, “Carol Davila” University of Medicine and Pharmacy, Bucharest, Romania

^c Department of Advanced Studies, “V. Babeş” National Institute of Pathology, Bucharest, Romania

^d Department of Dermatology, Colentina University Hospital, “Carol Davila” University of Medicine and Pharmacy, Bucharest, Romania

Received: March 2, 2012; Accepted: April 4, 2012

Abstract

Telocytes (TCs), a particular interstitial cell type, have been recently described in a wide variety of mammalian organs (www.telocytes.com). The TCs are identified morphologically by a small cell body and extremely long (tens to hundreds of μm), thin prolongations (less than 100 nm in diameter, below the resolving power of light microscopy) called telopodes. Here, we demonstrated with electron microscopy and immunofluorescence that TCs were present in human dermis. In particular, TCs were found in the reticular dermis, around blood vessels, in the perifollicular sheath, outside the glassy membrane and surrounding sebaceous glands, arrector pili muscles and both the secretory and excretory portions of eccrine sweat glands. Immunofluorescence screening and laser scanning confocal microscopy showed two subpopulations of dermal TCs; one expressed c-kit/CD117 and the other was positive for CD34. Both subpopulations were also positive for vimentin. The TCs were connected to each other by homocellular junctions, and they formed an interstitial 3D network. We also found TCs adjoined to stem cells in the bulge region of hair follicles. Moreover, TCs established atypical heterocellular junctions with stem cells (clusters of undifferentiated cells). Given the frequency of allergic skin pathologies, we would like to emphasize the finding that close, planar junctions were frequently observed between TCs and mast cells. In conclusion, based on TC distribution and intercellular connections, our results suggested that TCs might be involved in skin homeostasis, skin remodelling, skin regeneration and skin repair.

Keywords: telocytes • telopodes • skin • dermis • cell junctions • stem cells • mast cells • regeneration

Introduction

Telocytes (TCs) are a distinct population of interstitial cells that were recently identified in mammalian (and vertebrate) tissues [1–3]. Previously, TCs were unidentified, either because they were overlooked or because TCs were confused with other interstitial cell types, depending on the specific cellular inventory in a given organ. Currently, TCs have been identified in heart [4–8], lungs [9–11], skeletal muscle [12, 13], pleura [14], urinary tract [15], duodenum [16], jejunum [17], salivary glands [18], gallbladder [19], pancreas [20], placenta [21], myometrium [22, 23], mammary glands [24], the

meninges and choroid plexus [25] and the vasculature [6, 26, 27]. A study aimed to find TCs in skin was also recently reported [28].

The most specific ultrastructural feature of TCs is the presence of very long prolongations (several tens to hundreds of μm) called telopodes (Tps) [1]. A Tp comprises thin fibrillar-like segments (podomeres) in alternation with dilated, cistern-like regions (podoms), which accommodate mitochondria, elements of endoplasmic reticulum and caveolae. The podomere/podom structure gives Tps a moniliform aspect.

*Correspondence to: L. M. POPESCU, M.D., Ph.D.,
Department of Advanced Studies,
“V. Babeş” National Institute of Pathology,
Bucharest, Romania.
E-mail: imp@jcmm.org

Olga SIMIONESCU, M.D., Ph.D.,
1st Clinic of Dermatology, Carol Davila
University of Medicine and Pharmacy Colentina Hospital,
19-21 Stefan cel Mare Road, 020125 Bucharest, Romania.
Tel: +40740-614-342, +4021-410-84-87
Fax: +4031-417-56-72
E-mail: olgadana@yahoo.com

Typically, Tps interact with neighbouring cells, either directly, by cell-cell contact, which creates a 3D network, or indirectly, by shedding microvesicles or secreting paracrine signalling molecules, including microRNAs [6, 29, 30]. TCs cooperate with stem cells to form tandem cell structures [2], which are mostly found in stem cell niches of various organs [5, 6, 9, 12]. These tandem cell structures have been implicated in tissue regeneration and/or repair.

The dermis contains a rich population of resident cells, as demonstrated by electron microscopy and immunohistochemistry. Fibroblasts represent the most prominent and heterogeneous

population [31, 32], followed by macrophages, mast cells and a network of mesenchymal cells with dendritic morphology. Cells different from dermal fibroblasts, but morphologically similar to TCs, were previously described in the human dermis. These included antigen-presenting dermal dendrocytes [33, 34] and another intriguing 'dendritic-like' cell type, with a distinct CD34 positive phenotype, which, at that time, was called a 'dermal dendrite of type II' [35]. The precise nature and function of these cell types remain unclear, but they closely resemble TCs, both ultrastructurally and phenotypically.

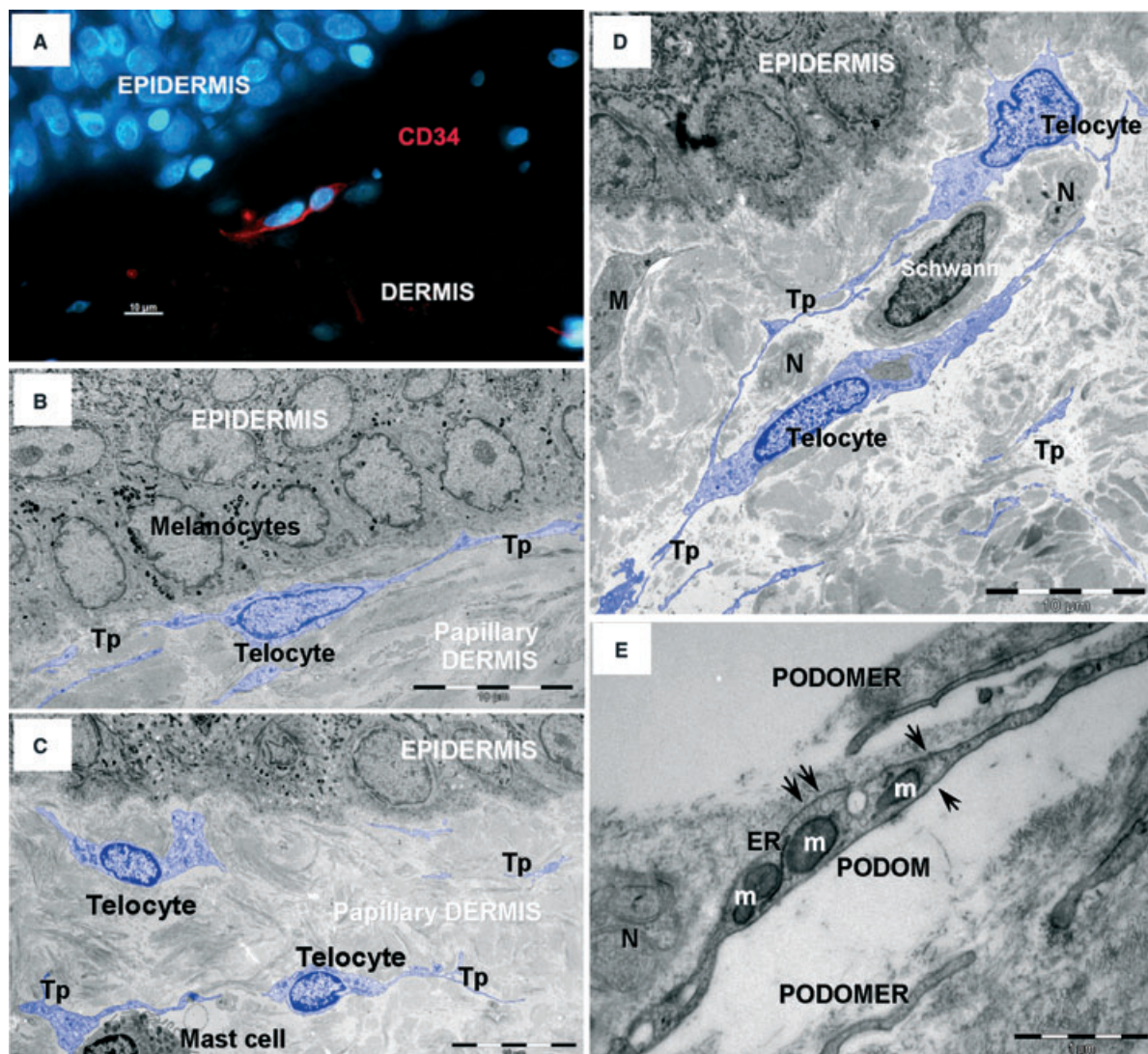


Fig. 1 Telocytes in human papillary dermis. (A) Epifluorescence microscopy – immunofluorescence labelling shows CD34 (red) interstitial cells. Nuclei are counterstained with DAPI (blue). Original magnification 400 \times . (B, C, D) Transmission electron microscopy (TEM) shows telocytes (coloured blue) with characteristic cellular processes – telopodes (Tps) – in papillary dermis. N – nerve endings; M – Macrophage. (E) TEM image shows detail of a telopode: thin segments (podomers) alternate with dilations (podoms) that contain mitochondria (m), endoplasmic reticulum (ER) and caveolae (arrows).

Fig. 2 Telocytes in human dermis. (A) Epifluorescence microscopy: Immunofluorescence shows the distribution of CD34 positive interstitial cells (red). This image reconstruction shows scarce CD34 positive cells (arrowheads) in the papillary dermis, under the epidermis and surrounding a sweat gland excretory duct and hair follicle infundibulum (i). Most CD34 positive cells populate the reticular dermis, concentrated around the hair follicle (HF). Original magnification 100×. (B, C and D) higher magnifications of boxed areas; (B) hair follicle infundibulum (i); (C) hair follicle bulge area (Bg); (D) sebaceous gland (SG) and arrector pili muscle (apm). Nuclei are counterstained with DAPI (blue). Original magnification 400×.

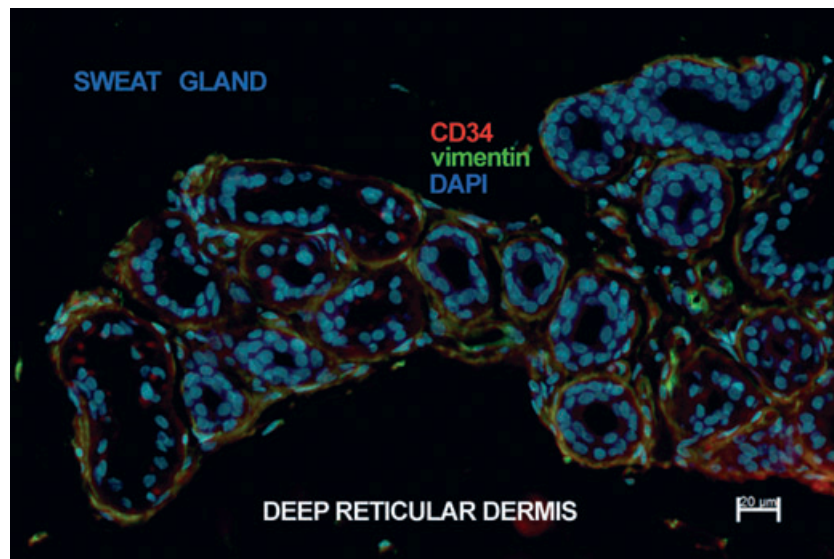
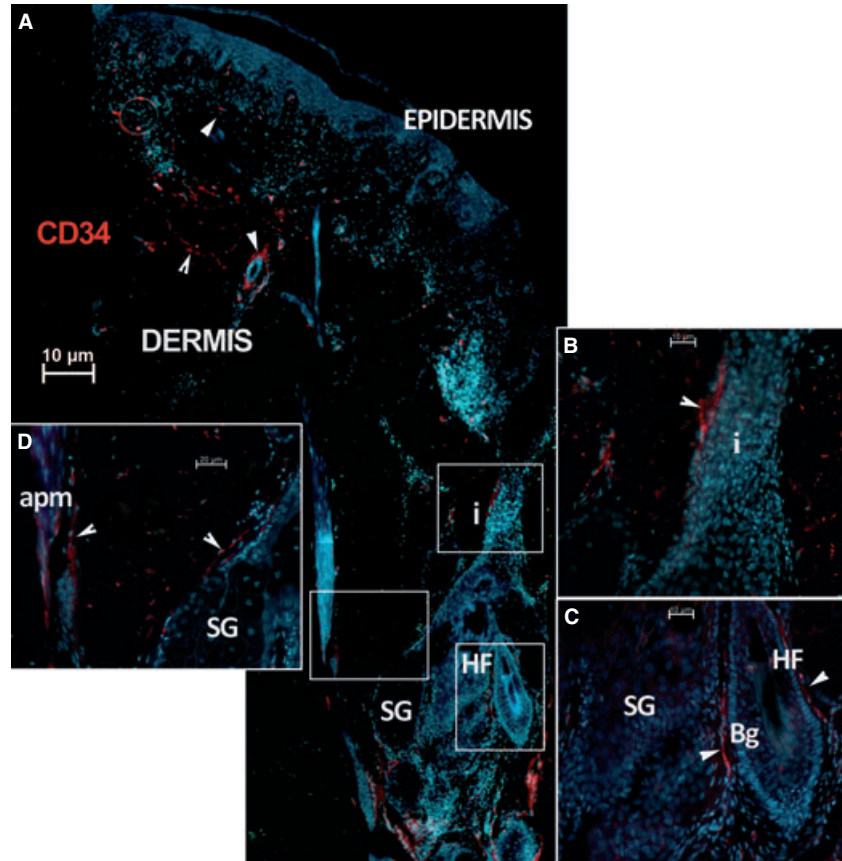


Fig. 3 Telocytes in human deep reticular dermis. Epifluorescence microscopy: double immunofluorescence labelling shows co-localization (yellow) of CD34 (red) and vimentin (green) in telocytes surrounding the secretory tubule and the initial excretory duct of the coiled segment of a sweat gland. Nuclei are counterstained with DAPI (blue). Original magnification 400×.

In this study, we used electron microscopy and immunohistochemistry to elucidate the existence of TCs in human dermis and to examine the nature of their close contacts (junctions) with dermal stem cells.

Materials and methods

Biopsies of human skin were obtained from three patients (informed written consent). Normal skin samples were obtained from a re-excision procedure after removing a local melanoma. The second excisions were performed according to the Breslow index (tumoural depth), 14 days after primary excision. The samples of normal skin were taken at 1 cm distance from primary suture. Experiments were performed according to the Helsinki guidelines, in full compliance with the Bioethics Committee of the 'Victor Babeş' National Institute of Pathology, Bucharest regulations.

In situ immunostaining and confocal analysis

Paraffin embedded skin samples (7µm thick) were deparaffinised, washed for 30 min. in PBS, pH 7.4 and blocked with 2% BSA. The samples were incubated for 30 min. with 2% normal goat serum (Sigma-Aldrich Chemical, St. Louis, MO, USA). Samples were incubated overnight at 4°C in PBS with either rabbit anti c-Kit or one of the following mouse monoclonal antibodies: anti-vimentin (clone V9, 1:150), anti- CD34 (clone QBEnd-10, 1:25) (both from Dako, Glostrup, Denmark) or anti-nestin (clone 10C2, 1:100) (Millipore, Billerica, MA, USA). In addition, combinations were used in double labelling assays. After washing in PBS with 0.1% (vol/vol) Triton X- 100, the sections were incubated with Alexa Fluor-conjugated, secondary goat anti-rabbit or goat antimouse antibodies (Invitrogen, Molecular Probes, Eugene, OR, USA) for another 2 hrs, at room temperature. Following an extensive washing step, the nuclei were stained with 1 µg/ml 4',6-diamidino-2-phenylindole (DAPI) (Sigma-Aldrich). Negative controls were performed by omitting the primary antibody from

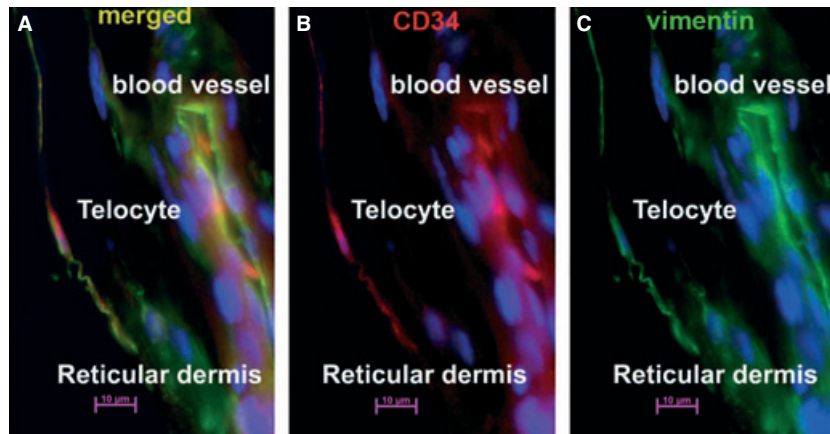


Fig. 4 Telocytes in human reticular dermis vasculature. Epifluorescence microscopy: double immunofluorescence labelling shows a telocyte located in the perivascular space of a blood vessel that (A) co-expresses CD34 and vimentin (yellow indicates merged colours) (B) CD34 label (red); (C) vimentin label (green). Nuclei are counterstained with DAPI (blue). Original magnification 400×.

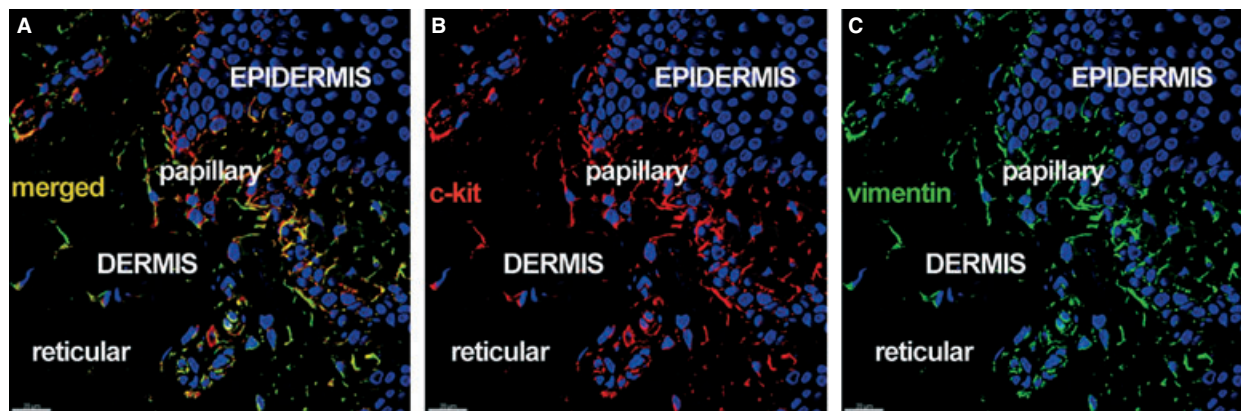


Fig. 5 Telocytes in human dermis. Laser scanning confocal microscopy: three-dimensional shadow projection image. Double immunofluorescence labelling shows (A) co-localization (yellow) of (B) CD117/c-kit (red), and (C) vimentin (green) in the stratum basale of the epidermis and in rare cells with telocyte morphology in the papillary dermis. Nuclei are counterstained with DAPI (blue). Original magnification 400×.

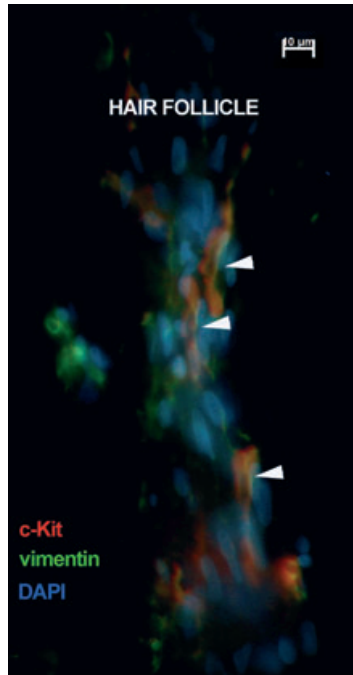


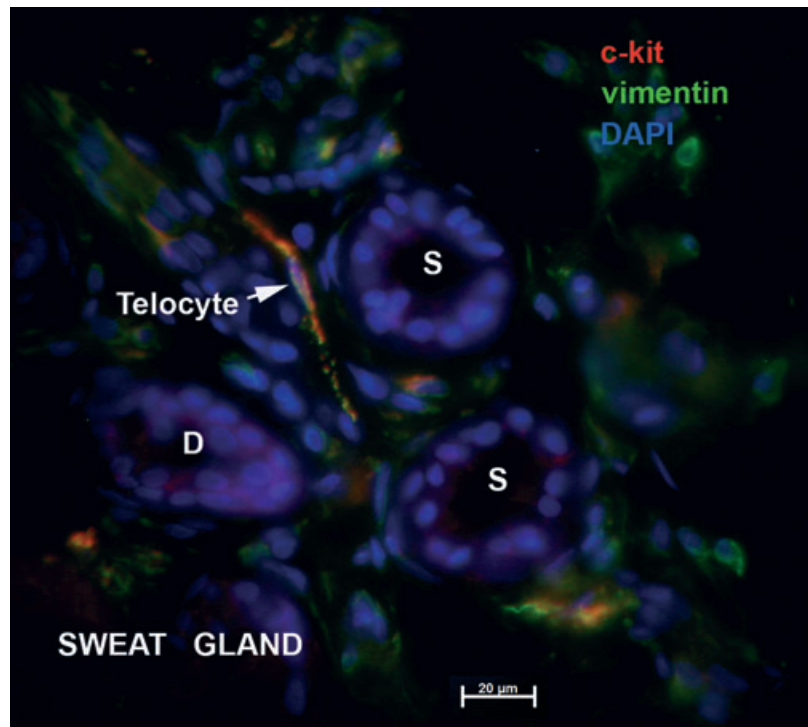
Fig. 6 Telocytes surrounding human hair follicle. Epifluorescence microscopy: double immunofluorescence labelling shows co-localization (yellow) of CD117/c-kit (red) and vimentin (green) in telocytes surrounding the hair follicle isthmus (arrowheads). Nuclei are counterstained with DAPI (blue). Original magnification 600 \times .

the same protocol. Epifluorescence was used to examine three to five immunolabelled sections from each biopsy on a Nikon Eclipse E600 microscope (Nikon Instruments Inc., Tokyo, Japan) with a Nikon Plan Apo 40 \times objective and the appropriate fluorescence filters. Digital pictures were acquired with a CCD Axiocam HRc Zeiss camera and AxioVision software (Carl Zeiss Imaging solution GmbH, Göttingen, Germany) or with confocal laser scanning microscopy, with a Nikon A1 laser microscope mounted on an ECLIPSE Ti-E inverted microscope. The confocal images were collected with a Plan Fluor 60 \times oil objective and 1.25-NA water (z-axis step 0.16 μ m). The following lasers and emission filters were used: Ar laser at 488 nm (used for the excitation of Alexa Fluor 488) and emission filter 500–550 nm; 561.2 nm G-HeNe laser (for Alexa Fluor 546) and emission filter 570–620 nm; and 405 nm Laser diode and 425–475 nm emission filter for DAPI. To improve the image quality, some original laser scanning microscopy data were subjected to digital deconvolution and three-dimensional reconstruction with an Imaris \times 64 (version 6.3.1.) from Bitplane AG (Zürich, Switzerland).

Transmission electron microscopy (TEM)

The TEM was performed on small (1 mm³) tissue fragments, processed according to a routine Epon-embedding procedure, as previously described [36]. Thin sections (about 60 nm) were examined with a Morgagni 286 transmission microscope (FEI Company, Eindhoven, The Netherlands) at 60 kV. Digital electron micrographs were acquired with a MegaView III CCD and iTEM-SIS software (Olympus, Soft Imaging System GmbH, Münster, Germany). To highlight the TCs and Tps, TEM images were digitally coloured in blue with Adobe[©] Photoshop CS3.

Fig. 7 Telocytes associated with human sweat gland. Epifluorescence microscopy: double immunofluorescence labelling shows co-localization (yellow) of CD117/c-kit (red) and vimentin (green) in a telocyte (arrow) found in between the coiled secretory tubule (S) and excretory duct (D) of a sweat gland in deep reticular dermis. Nuclei are counterstained with DAPI (blue). Original magnification 600 \times .



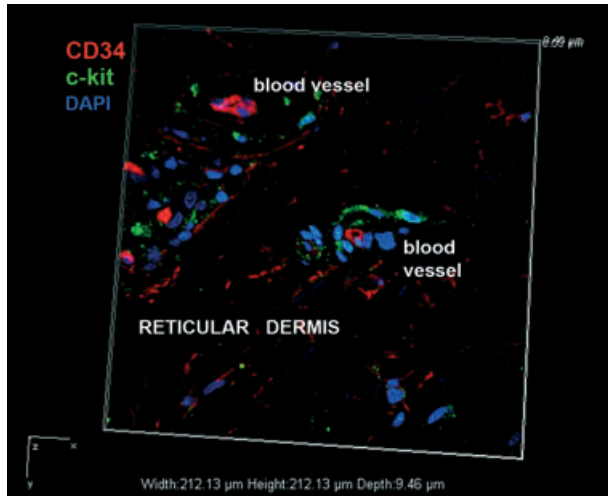


Fig. 8 Distinct subsets of interstitial cells in human dermis. Laser scanning confocal microscopy: volume reconstruction. Double immunofluorescence labelling shows distinct subsets of interstitial CD34 positive telocytes (red) and rare CD117/c-kit positive telocytes (green) scattered in the shallow reticular dermis or surrounding small blood vessels. Nuclei are counterstained with DAPI (blue). Original magnification 600 \times .

Results

Immunolabelling

Immunostaining revealed numerous CD34 positive cells in the connective tissue of human dermis. Most were endothelial cells, but there was also a large population of spindle-shaped cells, with long, very thin prolongations. These were presumably TCs, scattered between dermal collagen bundles. A few CD34 positive TCs were detected in the papillary dermis. These exhibited a bipolar shape with thin prolongations that extended parallel to the adjacent epidermis (Fig. 1A); they were concentrated around the spanning excretory ducts of eccrine sweat glands, blood vessels and the infundibulum of hair follicles (Fig. 2A,B). Most CD34 positive TCs were identified in the reticular dermis, where they formed a network around the deep segments of hair follicles, in the bulge and sub-bulge areas (Fig. 2A,C). They also surrounded sebaceous glands and arrector pili muscles (Fig. 2D). In addition, CD34 positive TCs were found in the deep dermis, around the secretory and the ductal parts of eccrine sweat glands (Fig. 3). The CD34 dermal TCs were frequently detected in the perivascular connective tissue, accompanying small and intermediate blood vessels (Fig. 4).

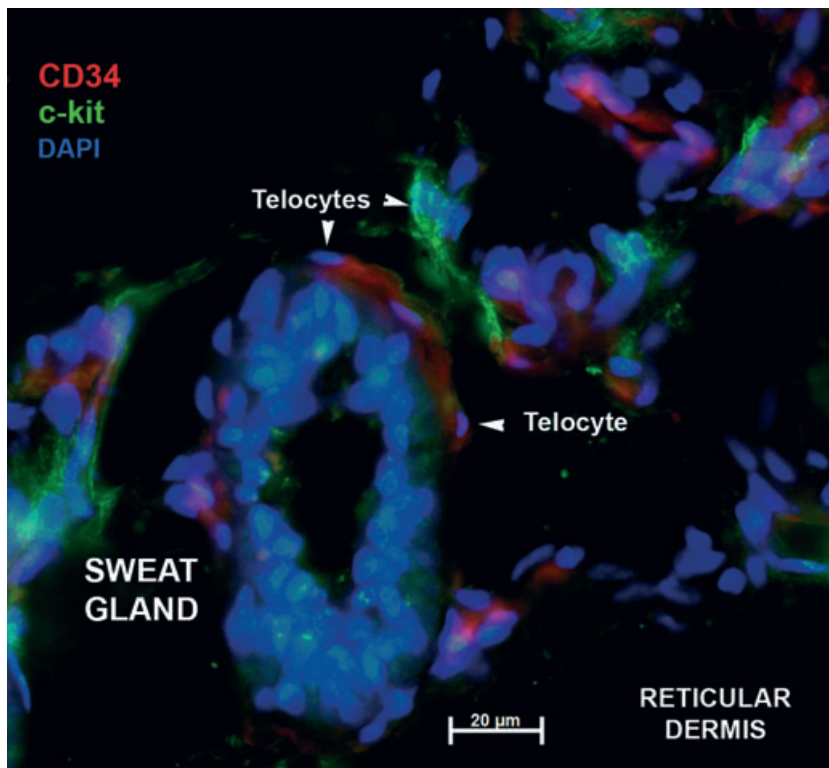


Fig. 9 Distinct subsets of telocytes in connective tissue around sweat gland. Epi-fluorescence microscopy: double immunofluorescence labelling shows distinct CD117/c-kit (green) and CD34 (red) telocytes (arrows) in the connective tissue surrounding the secretory tubule (S) of a sweat gland from deep reticular dermis. Nuclei are counterstained with DAPI (blue). Original magnification 600 \times .

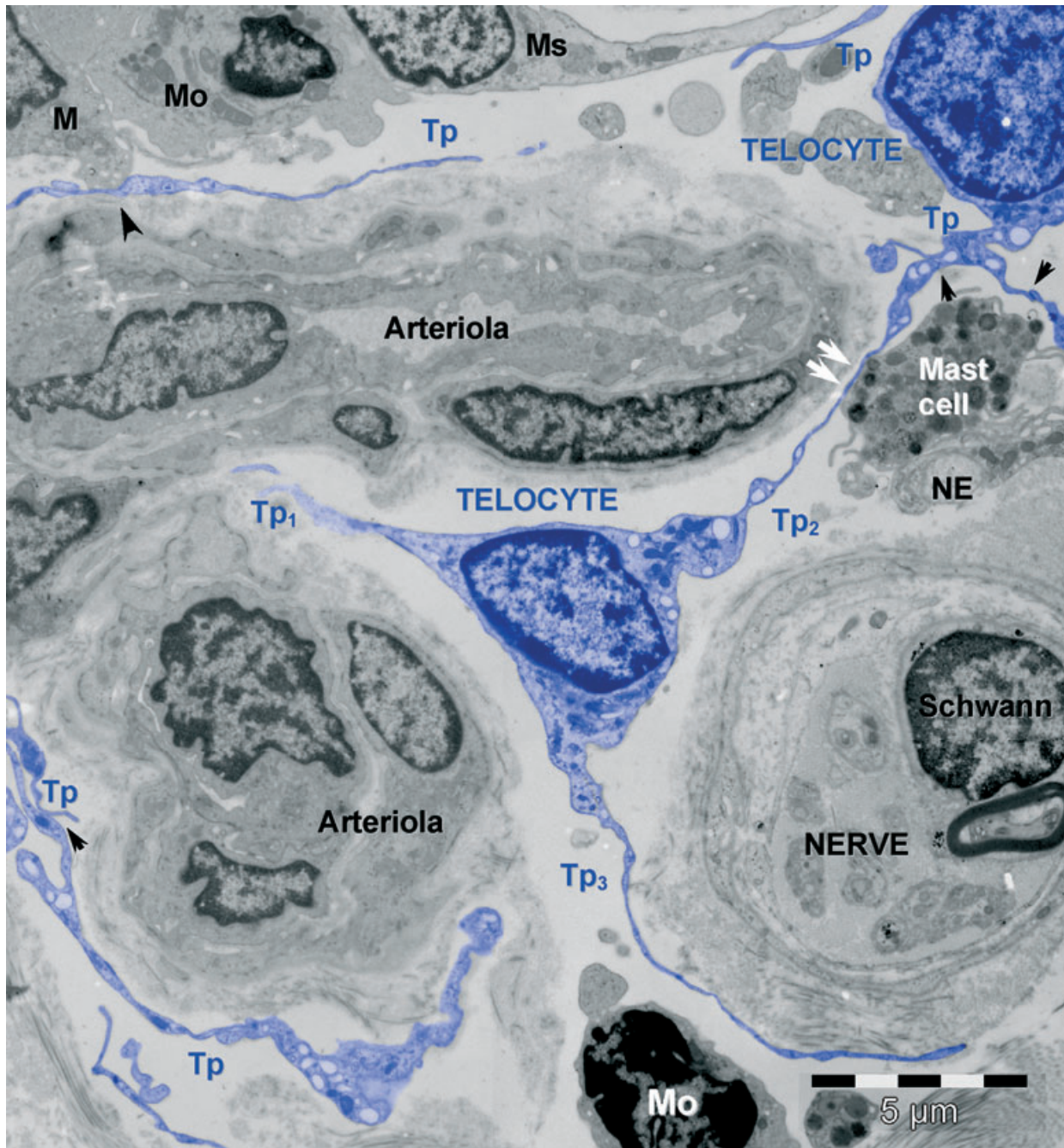


Fig. 10 Telocytes form an interstitial network in human dermis. Digitally enhanced (blue colour) TEM image shows telocytes (blue) with telopodes (Tp). Telocytes are connected by junctions (black arrows; see detailed image in Fig. 16A). The telocyte in the centre of image has three telopodes (Tp₁–Tp₃) extended between arterioles and nerves. Note close contacts between a Tp and macrophages (M) (black arrowhead) and a Tp and mast cell (white arrows, see detailed image in Fig. 17C). Mo – mononuclear cells; Ms – mesenchymal cell; NE – nerve ending.

We also detected c-kit/CD117 expression in cells with TC morphology, located either in the papillary dermis (Fig. 5) or in the connective tissue surrounding skin adnexal structures, like the hair follicle (Fig. 6) and sweat glands (Fig. 7).

Double immunostaining for CD34 and c-kit clearly showed two distinct subsets of cells with TC morphology that expressed either CD34 or c-kit; these subsets had similar distributions in the papillary (Fig. 8) and reticular (Fig. 9) dermis,

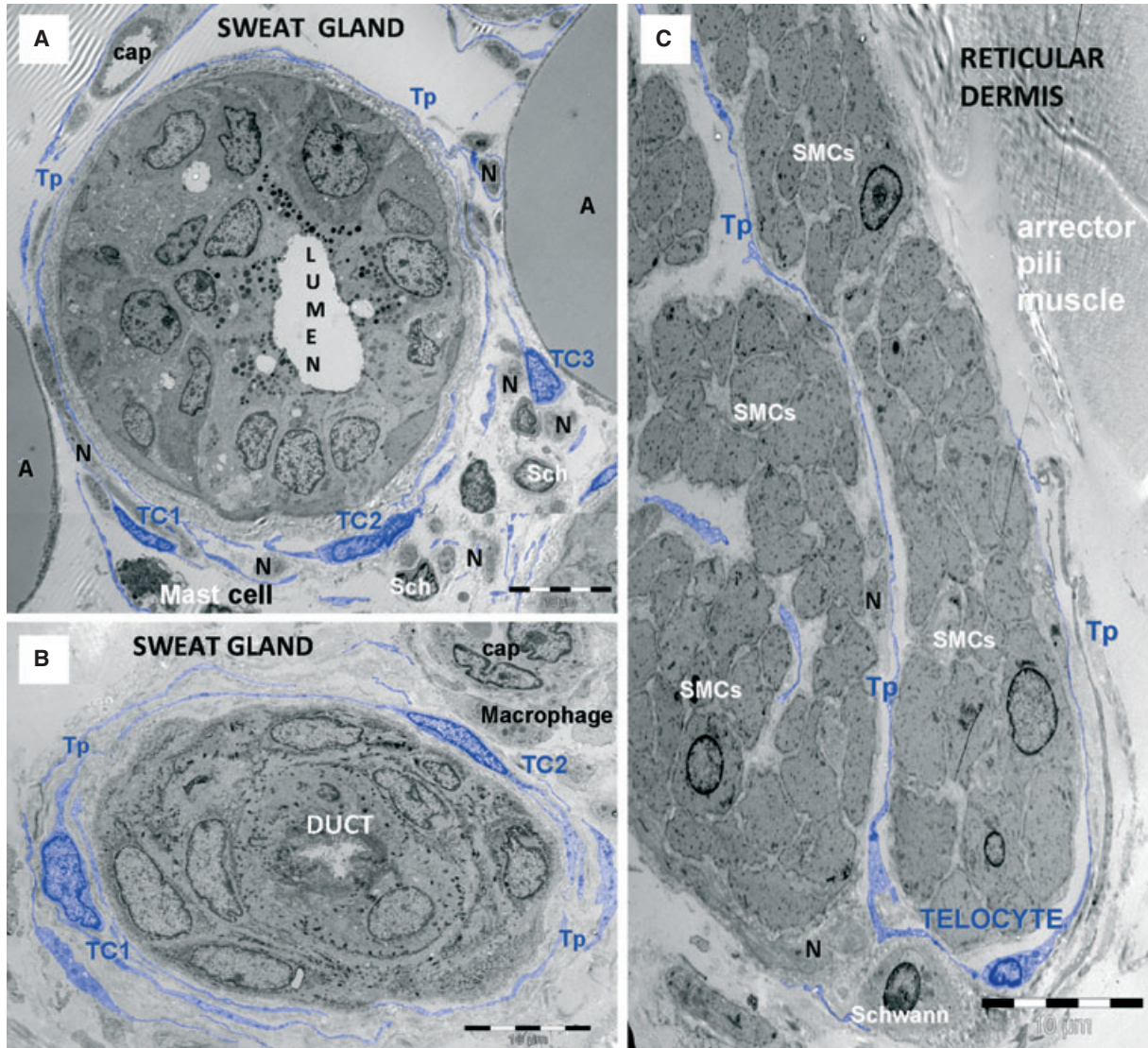


Fig. 11 Telocytes form a sheath around human sweat gland. TEM micrographs show telocytes (TC1–TC3) with their telopodes (Tp) (A) enfolding the sweat gland, (B) its excretory duct and (C) arrector pili muscle fascicles. SMCs – smooth muscle cells. Note Schwann cells (Sch), nerve endings (N), mast cells, capillaries (cap), macrophages and adipocytes (A).

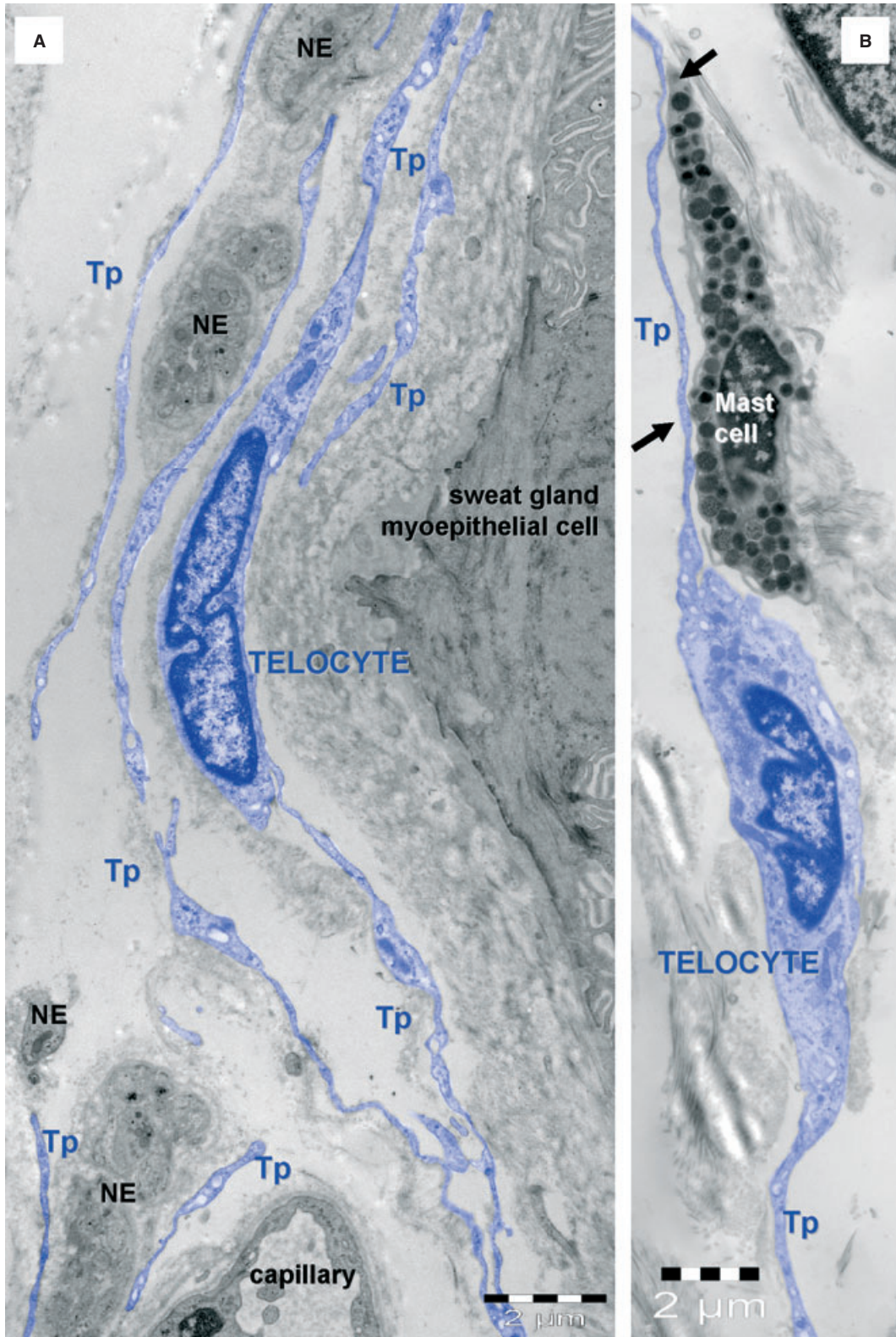
demonstrated by the co-expression of vimentin intermediate filaments (Figs 3–7).

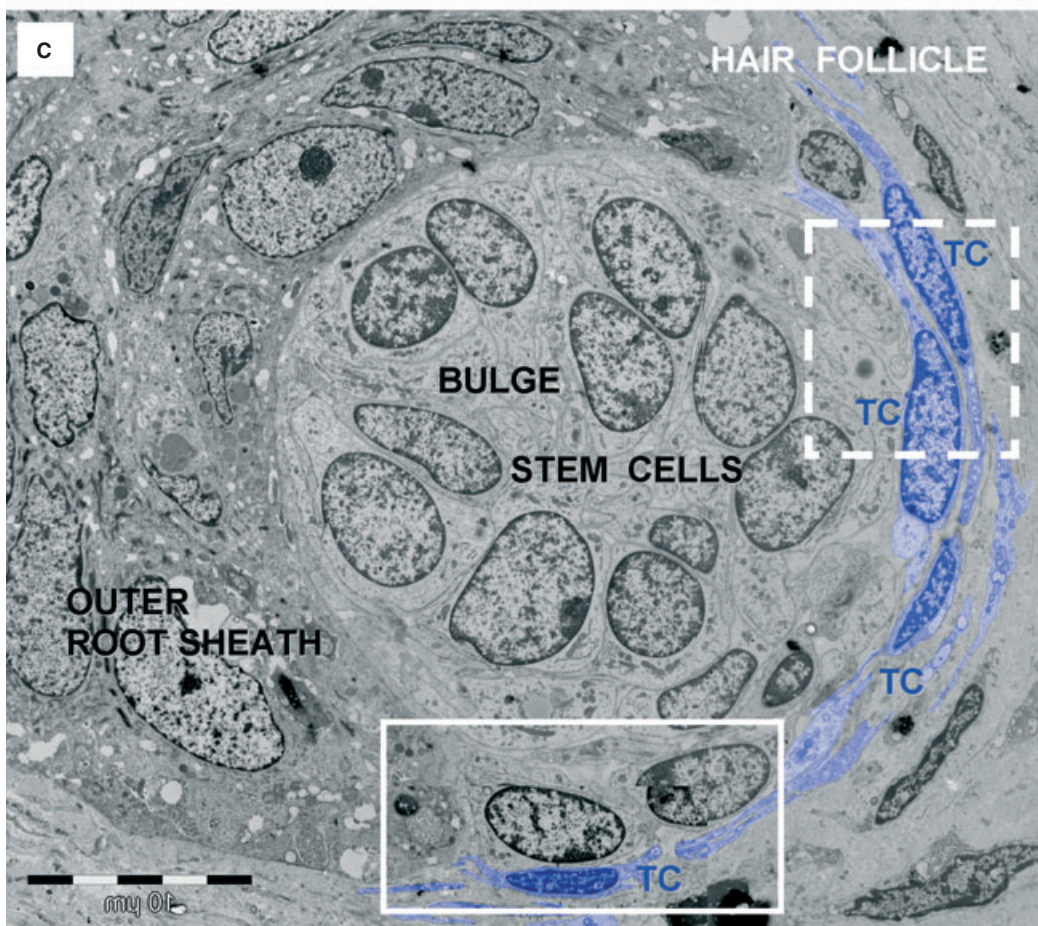
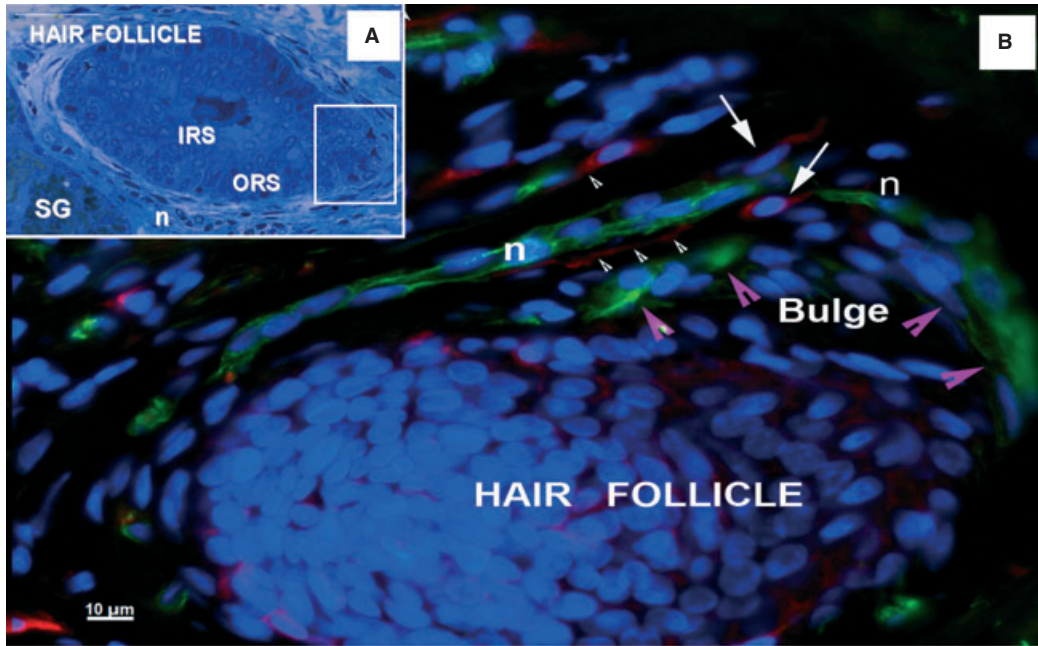
TEM

The TEM analysis was focused on dermal connective tissue. Immunohistochemistry showed CD34 or c-kit positive cells around

the hair follicles, blood vessels and the secretory and excretory parts of eccrine sweat glands. The TEM images showed that all these structures were surrounded by interstitial cells with TC morphology (Figs 10–15), elongated cells with two or three long cellular processes (Tps; Figs 1, 10–17). The TCs had little cytoplasm with few organelles, like mitochondria and endoplasmic reticulum. The Tps (Figs 10–17) were long ($46.37 \pm 12.63 \mu\text{m}$; range: 29.88–74.52 μm) and very thin (mean diameter:

Fig. 12 Telocyte layers in human skin appendages. (A) Telocytes (blue) form layers around an eccrine sweat gland mixed with nerve endings (NE). (B) Telocytes are typically associated with mast cells. Tp – telopodes.





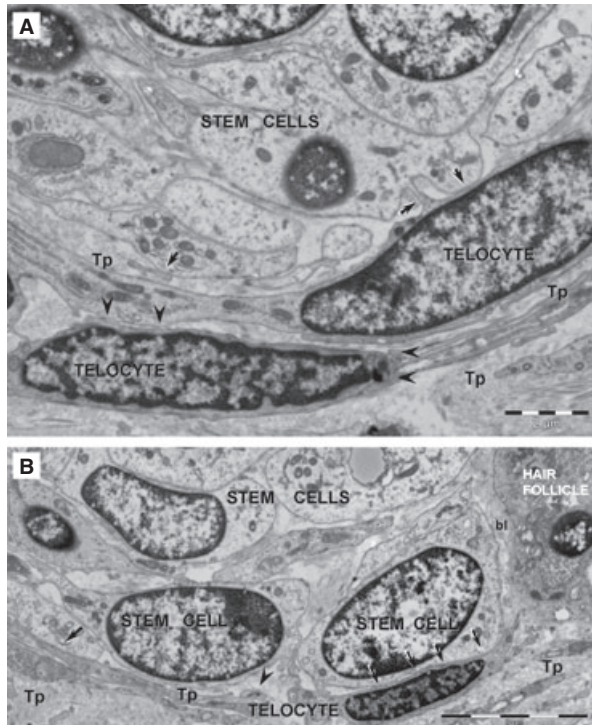


Fig 14 Telocytes bordering stem cells. High magnification TEM images of the boxed areas in Fig. 13 C. The dashed-line box is magnified in (A); the continuous-line box is magnified in (B). Two layers of interconnected telocytes (arrowheads) were found bordering stem cells. Telocytes formed point contacts (arrows in A) or planar contacts (arrowheads in B) with stem cells. Undifferentiated stem cells have few mitochondria, endoplasmic reticulum cisternae, and numerous free ribosomes. The basal lamina (bl) of the hair follicle is visible between epidermal cells in outer root sheath and stem cells.

90.86 ± 30.79 nm; range: 47.40–129.51 nm). The moniliform aspect of Tps, or the uneven calibre (Figs 1, 10–12), was due to an irregular alternation between the thin podomere segments (diameter, 40–100 nm), and dilated podoms (diameter, 200–500 nm or more), which contained mitochondria, endoplasmic reticulum and caveolae (Fig. 1E).

The TEM images confirmed that TCs were scarce in the papillary dermis (Fig. 1), but numerous in the reticular dermis, where they wrapped around blood vessels (Fig. 10), sweat glands (Figs 11A, 13B), excretory ducts of sweat glands (Fig. 11B), arrector pili muscle fascicles (Fig. 11C) and the hair follicle (Figs 13–15). Typically, two

or three layers of TCs formed an incomplete sheath that wrapped around skin adnexa (Figs 11, 13).

The TCs were connected to each other by homocellular junctions to form an interstitial network (Fig. 16). These junctions were typically *puncta adhaerentia minima* or *recessus adhaerens*, but gap junctions were also observed. Heterocellular junctions (planar contacts or point contacts) were found connecting TCs and mast cells or mononuclear cells (Fig. 17).

TCs and stem cells

The TCs were found bordering a round cluster of undifferentiated cells (stem cells) in the bulge regions of hair follicles (Figs 13, 14). The stem cells showed large euchromatic nuclei, few mitochondria, few endoplasmic reticulum cisternae and numerous free ribosomes (Fig. 14B). The stem cells were not connected to each other by classical junctions (only small immature *adhaerentes* junctions were found); and they were not connected with cells from the outer root sheath. However, point contacts (Fig. 14A) and planar contacts (Fig. 14B) were observed between TCs and stem cells. We screened for stem cell clusters in the bulge areas by immunolabelling for nestin. This revealed small, oval-shaped, nestin-expressing cells in the outer root sheath of the bulge area. C-kit/CD117 positive TCs were spotted around the nestin positive stem cells, intercalated between the bulge areas of hair follicles and the adjoining nerve fibres (Fig. 13B).

Discussion

The present study showed that TCs represented a distinct population of cells. They were distinguished by their particular distribution and their immunophenotypes, which differentiated them from other skin cells. Two subpopulations of TCs were detected in the normal human dermis, based on specific marker expression of CD34 or c-kit. The TCs were present around vascular structures, nerves, smooth muscle bundles and adnexal structures, including the bulge regions of the hair follicles.

In the last two decades, several authors described the presence of CD34 positive stromal cells within the dermis [37]. At first, these studies were purely descriptive, and the histogenesis and putative function of this cell population remained enigmatic. Subsequent studies suggested that dermal CD34 positive interstitial cells were derived, at least partly, from circulating fibrocytes, were capable of tissue invasion and were implicated in wound healing [38].

Fig. 13 Telocytes around human hair follicle and adjacent sebaceous gland. (A) Light microscopy image of toluidine-blue coloured, thin section shows a hair follicle and an adjacent sebaceous gland (SG). IRS: inner root sheath; ORS: outer root sheath; n: perifollicular nerve fibres. (B) Epifluorescence microscopy: double labelling shows nestin positive cells (green), stem cells from the bulge area of hair follicle (magenta arrowheads) and perifollicular nerve fibres (N), surrounded by CD117 positive TCs (red, white arrows) with long telopodes (white arrowhead). Nuclei are counterstained with DAPI (blue). Original magnification 400×. (C) TEM of the boxed area in (A) shows a cluster of stem cells in the outer root sheath of a hair follicle. The stem cells are bordered by telocytes (TC) with telopodes, and other cells from the outer root sheath. Boxed areas are enlarged in Fig. 14.

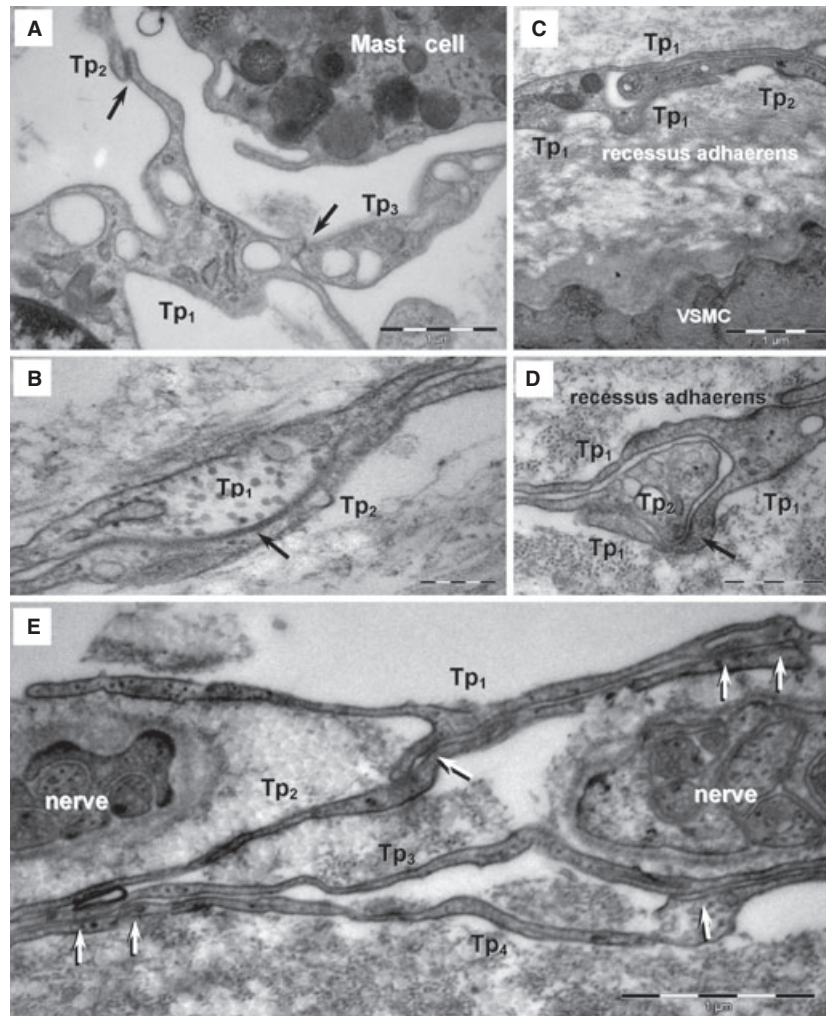


Fig 16 Homocellular junctions between telocytes in human skin (TEM). **(A)** Three telopodes (Tp₁–Tp₃) are connected by small adherens junctions (arrows). **(B)** A gap junction is visible between two telopodes (Tp₁, Tp₂). **(C, D)** The telopode (Tp₁) of one telocyte embraces the cytoplasmic extension (Tp₂) of another telocyte, forming a *recessus adhaerens*. A *punctum adhaerentia minimum* is visible in **D** (arrow). VSMC – vascular smooth muscle cell. **(E)** Overlapping telopodes (Tp₁–Tp₄) are connected by *puncta adhaerentia minima* (arrows).

Mouse hair follicle stem cells have been shown to express CD34, but in human, its expression pattern remains controversial. Ohyama *et al.* [39] showed that CD34 was expressed in the non-bulge outer root sheath; Raposio *et al.* [40] reported CD34 expression in the bulge area; Jiang *et al.* [41] reported expression in the basal layer of the interfollicular epidermis; and Trempus *et al.* showed expression in mouse keratinocytes in the hair follicle bulge [42]. These cells, identified by immunophenotype, were also found around microvessels of perifollicular regions, which represent a niche for mesenchymal stem cells, in human scalp skin [43]. Our data showed no CD34 positive staining in the epidermis, weak CD34 staining in the hair follicle outer sheath and some CD34 expression outside the outer root sheath in the infundibular, bulge and sub-bulge zones.

During embryogenesis, c-kit signalling is important for melanoblast and/or melanocyte migration, proliferation and differentiation; in addition, c-kit contributes to maintaining postnatal cutaneous melanogenesis [44, 45]. However, its role in epidermal and hair follicle regeneration remains unknown. Consistent with previous studies[41], we detected c-kit in the rete ridges of the epidermis (*stratum basale*), melanocytes, mast cells, the outermost layer of the infundibulum and in the hair matrix.

The major obstacle in identifying TCs with light microscopy is that they are morphologically similar to different types of so called ‘fibroblast-like’ or ‘dendritic-like’ stromal cells. In this study, we used double immunohistochemical staining to distinguish TCs from other skin cells.

Fig 15 Telocytes associated with nerve endings. TEM image shows telocytes and numerous telopodes (Tp) next to nerve endings (N) that are present in the dermal papilla of a hair follicle. The inset image shows the hair follicle at low magnification; the boxed area was enlarged to show telocyte details.

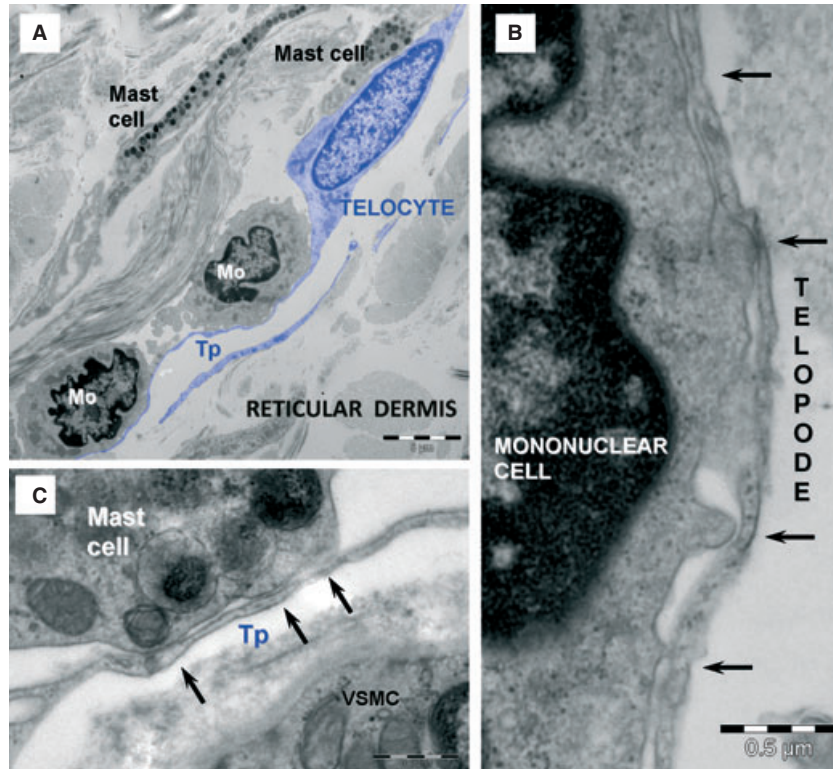


Fig 17 Heterocellular contacts between telocytes and other interstitial cells. (A) TEM image shows telocytes (coloured blue), mononuclear cells (Mo) and mast cells. (B) High magnification of the contact area in (A) shows a planar contact between a telopode (Tp) and a mononuclear cell in the reticular dermis. (C) High magnification of a telopode (Tp) that formed point contacts (arrows) with a mast cell. (Detail of the heterocellular connection marked with white arrows in Fig. 10);VSMC – vascular smooth muscle cell.

Unlike Langerhans cells, c-kit and CD34 positive TCs did not express CD1a, and they did not contain Birbeck granules. However, anti-CD1a antibodies labelled intraepidermal and rare dermal Langerhans cells (data not shown). Unlike other dermal dendritic cells, TCs did not express CD36 or CD11a, and they were predominantly located in the reticular dermis, rather than the papillary dermis. Furthermore, most c-kit positive cells with TC morphology did not express mast cell tryptase in double immunostaining experiments (data not shown). However, it was sometimes difficult to assess differential expression of c-kit and tryptase, most likely because mast cells and TCs were sometimes closely apposed, particularly in the papillary dermis (Fig. 12B). Unlike myofibroblasts, TCs did not express alpha smooth muscle actin, and they did not form myofilaments or fibronexus junctions with the extracellular matrix. Finally, TCs could be distinguished from ordinary fibroblasts, because they did not express procollagen or CD90.

The particular network-like arrangement of TCs, based on homotypic (TC–TC junctions) and heterocellular interactions, supported the notion that they may perform intercellular signalling. Thus, they may convert the interstitium into an integrated system that contributes to maintaining organ homeostasis.

The close apposition between TCs and mast cells was frequently observed in other organs that harboured TCs [6, 46–48]. In some studies, a stromal synapse was described [48]. This type of cooperation might suggest that TCs were involved in either activation or repression of mast cells during allergic reactions [49]. However, the precise nat-

ure of this intercellular relationship and the pathogenic mechanism underlying different pathological states require further study.

The TCs have been spotted in the vicinity of several types of progenitors in various organs, like the heart [5], lungs [9] and skeletal muscles [12]. Our observations of TC distributions and interactions in human skin supported the notion that TCs are members of the stem cell niches, and may play the role of ‘nurse’ cells for adjacent mesenchymal and epithelial stem cells. Multiple stem and progenitor cell compartments have been identified in both dermal connective tissues and the epidermis. In the dermal layer, mesenchymal stem cells have been identified in the follicular connective sheath and the papilla [50–52]. In the human epidermis, there are at least two distinct stem cell compartments. Both compartments contain slow-cycling cells with high proliferative potential, and we found that both were guarded by TCs. One of these compartments was the basal layer of the interfollicular epidermis [53]; the other, was the bulge of the hair follicle. The latter is the best characterized stem cell compartment; it comprises a specific microenvironment, called the stem cell niche [54, 55], located between the opening duct of the sebaceous gland and the attachment point of arrector pili muscle. This area is responsible for the regeneration of the pilosebaceous unit, but it does not possess a distinctive morphology in humans [41, 56]. Thus, stem cells at this level are not morphologically distinct, but they exhibit a specific array of markers, including nestin [57]. According to the ‘bulge activation hypothesis’, bulge stem cells will proliferate and differentiate only after receiving signals from specialized adjacent stromal cells [58]. Potential sources

of stem cells include the epithelial stem cells in the epidermis and hair follicle and those in other skin adnexa, like the sebaceous glands and sweat glands [59, 60]. Sebaceous gland homeostasis requires a population of progenitor cells that constantly gives rise to differentiating cells that are eliminated through the hair canal. Lineage tracing suggested that a small population of cells near the base of the sebaceous gland might be stem cells [61]. We detected CD34 positive TCs in close contact with both sebaceous and sweat glands.

The existence of different skin stem cell compartments and the ability of these niches to respond differentially to environmental signals remain exciting topics in the field. The TC represents a new player in the composition of various niches, and they should not be overlooked. In our opinion, the presence of TCs represents potential indirect (chemical) and/or direct (junctional) contacts with resident stem cells that could increase the efficiency and efficacy of repair and regeneration processes.

References

1. **Popescu LM, Faussone-Pellegrini MS.** TELOCYTES – a case of serendipity: the winding way from Interstitial Cells of Cajal (ICC), via Interstitial Cajal-Like Cells (ICLC) to TELOCYTES. *J Cell Mol Med.* 2010; 14: 729–40.
2. **Popescu LM.** The Tandem: telocytes – stem cells. *Int J Biol Biomed Eng.* 2011; 5: 83–92.
3. **Faussone-Pellegrini MS, Popescu LM.** Telocytes. *Biomol Concepts.* 2011; 2: 481–9.
4. **Popescu LM, Manole CG, Gherghiceanu M, et al.** Telocytes in human epicardium. *J Cell Mol Med.* 2010; 14: 2085–93.
5. **Gherghiceanu M, Popescu LM.** Cardiomyocyte precursors and telocytes in epicardial stem cell niche: electron microscope images. *J Cell Mol Med.* 2010; 14: 871–7.
6. **Gherghiceanu M, Popescu LM.** Cardiac telocytes – their junctions and functional implications. *Cell Tissue Res.* 2012; doi: 10.1007/s00441-012-1333-8
7. **Gherghiceanu M, Manole CG, Popescu LM.** Telocytes in endocardium: electron microscope evidence. *J Cell Mol Med.* 2010; 14: 2330–4.
8. **Rusu MC PF, Hostiuc S, Hostiuc S, et al.** Telocytes form networks in normal cardiac tissues. *Histol Histopathol.* 2012; 27: 807–16.
9. **Popescu LM, Gherghiceanu M, Suciu LC, et al.** Telocytes and putative stem cells in the lungs: electron microscopy, electron tomography and laser scanning microscopy. *Cell Tissue Res.* 2011; 345: 391–403.
10. **Zheng Y, Bay C, Wang X.** Telocyte morphologies and potential roles in diseases. *J Cell Physiol.* 2012; 227: 2311–7.
11. **Zheng Y, Bay C, Wang X.** Potential significance of telocytes in the pathogenesis of lung diseases. *Expert Rev Respir Med.* 2012; 6: 45–9.
12. **Popescu LM, Manole E, Serboiu CS, et al.** Identification of telocytes in skeletal muscle interstitium: implication for muscle regeneration. *J Cell Mol Med.* 2011; 15: 1379–92.
13. **Suciu LC, Popescu BO, Kostin S, Popescu LM.** PDGFR-beta positive telocytes in skeletal muscle interstitium. *J Cell Mol Med.* 2012; 16: 701–7.
14. **Hinescu ME, Gherghiceanu M, Suciu L, Popescu LM.** Telocytes in pleura: two- and three-dimensional imaging by transmission electron microscopy. *Cell Tissue Res.* 2011; 343: 389–97.
15. **Gevaert T, De Vos R, Van Der Aa F, et al.** Identification of telocytes in the upper lamina propria of the human urinary tract. *J Cell Mol Med.* 2012; doi:10.1111/j.1582-4934.2011.01504.x
16. **Cantarero Carmona I, Luesma Bartolome MJ, Junquera Escribano C.** Identification of telocytes in the lamina propria of rat duodenum: transmission electron microscopy. *J Cell Mol Med.* 2011; 15: 26–30.
17. **Cretoiu D, Cretoiu SM, Simionescu AA, Popescu LM.** Telocytes, a distinct type of cell among the stromal cells present in the lamina propria of jejunum. *Histol Histopathol.* 2012; doi: http://dx.doi.org/10.1016/j.neulet.2012.04.006.
18. **Nicolescu MI, Bucur A, Dinca O, et al.** Telocytes in parotid glands. *Anat Rec.* 2012; 295: 378–85.
19. **Hinescu ME, Ardeleanu C, Gherghiceanu M, Popescu LM.** Interstitial Cajal-like cells in human gallbladder. *J Mol Histol.* 2007; 38: 275–84.
20. **Nicolescu MI, Popescu LM.** Telocytes in the interstitium of human exocrine pancreas: ultrastructural evidence. *Pancreas.* 2012; doi: 10.1097/MPA.0b013e31823fbded.
21. **Suciu L, Popescu LM, Gherghiceanu M, et al.** Telocytes in human term placenta: morphology and phenotype. *Cells Tissues Organs.* 2010; 192: 325–39.
22. **Popescu LM, Vidulescu C, Curici A, et al.** Imatinib inhibits spontaneous rhythmic contractions of human uterus and intestine. *Eur J Pharmacol.* 2006; 546: 177–81.
23. **Cretoiu SM, Simionescu AA, Caravia L, et al.** Complex effects of imatinib on spontaneous and oxytocin-induced contractions in human non-pregnant myometrium. *Acta Physiol Hung.* 2011; 98: 329–38.
24. **Gherghiceanu M, Popescu LM.** Interstitial Cajal-like cells (ICLC) in human resting mammary gland stroma. Transmission electron microscope (TEM) identification. *J Cell Mol Med.* 2005; 9: 893–910.
25. **Popescu BO, Gherghiceanu M, Kostin S, et al.** Telocytes in meninges and choroid plexus. *Neurosci Lett.* 2012; in press; doi: http://dx.doi.org/10.1016/j.neulet.2012.04.006.
26. **Gherghiceanu M, Hinescu ME, Andrei F, et al.** Interstitial Cajal-like cells (ICLC) in myocardial sleeves of human pulmonary veins. *J Cell Mol Med.* 2008; 12: 1777–81.
27. **Cantarero I, Luesma MJ, Junquera C.** The primary cilium of telocytes in the vasculature: electron microscope imaging. *J Cell Mol Med.* 2011; 15: 2594–600.
28. **Rusu MC, Mirancea N, Manoiu VS, et al.** Skin telocytes. *Ann Anat.* 2012; doi:10.1016/j.aanat.2011.11.007.
29. **Cismasiu VB, Radu E, Popescu LM.** miR-193 expression differentiates telocytes from other stromal cells. *J Cell Mol Med.* 2011; 15: 1071–4.
30. **Manole CG, Cismasiu V, Gherghiceanu M, Popescu LM.** Experimental acute myocardial infarction: telocytes involvement in neo-angiogenesis. *J Cell Mol Med.* 2011; 15: 2284–96.
31. **Sorrell JM, Caplan AI.** Fibroblast heterogeneity: more than skin deep. *J Cell Sci.* 2004; 117: 667–75.
32. **Bergstresser PR, Costner MI.** Anatomy and Physiology. In: Bologna J, Jorizzo JL, Rapini RP, editors. *Dermatology.* 2nd ed. St Louis: Mosby; 2008: p. 25–35
33. **Headington JT.** The dermal dendrocyte. *Adv Dermatol.* 1986; 1: 159–71.
34. **Cerio R, Griffiths CE, Cooper KD, et al.** Characterization of factor XIIIa positive dermal dendritic cells in normal and inflamed skin. *Br J Dermatol.* 1989; 121: 421–31.
35. **Nickoloff BJ.** The human progenitor cell antigen (CD34) is localized on endothelial cells, dermal dendritic cells, and perifollicular cells in formalin-fixed normal skin, and on proliferating endothelial cells and stromal

- spindle-shaped cells in Kaposi's sarcoma. *Arch Dermatol.* 1991; 127: 523–9.
36. **Mandache E, Popescu LM, Gherghiceanu M.** Myocardial interstitial Cajal-like cells (ICLC) and their nanostructural relationships with intercalated discs: shed vesicles as intermediates. *J Cell Mol Med.* 2007; 11: 1175–84.
 37. **Narvaez D, Kanitakis J, Faure M, Claudy A.** Immunohistochemical study of CD34-positive dendritic cells of human dermis. *Am J Dermatopathol.* 1996; 18: 283–8.
 38. **Bucala R, Spiegel LA, Chesney J, et al.** Circulating fibrocytes define a new leukocyte subpopulation that mediates tissue repair. *Mol Med.* 1994; 1: 71–81.
 39. **Ohyama M, Terunuma A, Tock CL, et al.** Characterization and isolation of stem cell-enriched human hair follicle bulge cells. *J Clin Invest.* 2006; 116: 249–60.
 40. **Raposio E, Guida C, Baldelli I, et al.** Characterization of multipotent cells from human adult hair follicles. *Toxicol In Vitro.* 2007; 21: 320–3.
 41. **Jiang S, Zhao L, Purandare B, Hantash BM.** Differential expression of stem cell markers in human follicular bulge and interfollicular epidermal compartments. *Histochem Cell Biol.* 2010; 133: 455–65.
 42. **Trempus CS, Morris RJ, Bortner CD, et al.** Enrichment for living murine keratinocytes from the hair follicle bulge with the cell surface marker CD34. *J Invest Dermatol.* 2003; 120: 501–11.
 43. **Krause DS, Ito T, Fackler MJ, et al.** Characterization of murine CD34, a marker for hematopoietic progenitor and stem cells. *Blood.* 1994; 84: 691–701.
 44. **Botchkareva NV, Khlgatian M, Longley BJ, et al.** SCF/c-kit signaling is required for cyclic regeneration of the hair pigmentation unit. *FASEB J.* 2001; 15: 645–58.
 45. **Hachiya A, Kobayashi A, Yoshida Y, et al.** Biphasic expression of two paracrine melanogenic cytokines, stem cell factor and endothelin-1, in ultraviolet B-induced human melanogenesis. *Am J Pathol.* 2004; 165: 2099–109.
 46. **Rusu MC, Jianu AM, Mirancea N, et al.** Tracheal telocytes. *J Cell Mol Med.* 2012; 16: 401–5.
 47. **Zheng Y, Li H, Manole CG, Sun A, et al.** Telocytes in trachea and lungs. *J Cell Mol Med.* 2011; 15: 2262–8.
 48. **Popescu LM, Gherghiceanu M, Cretoiu D, Radu E.** The connective connection: interstitial cells of Cajal (ICC) and ICC-like cells establish synapses with immunoreactive cells. Electron microscope study *in situ.* *J Cell Mol Med.* 2005; 9: 714–30.
 49. **Cozzi E, Ackerman KG, Lundquist A, et al.** The naive airway hyperresponsiveness of the A/J mouse is Kit-mediated. *Proc Natl Acad Sci USA.* 2011; 108: 12787–92.
 50. **Lako M, Armstrong L, Cairns PM, et al.** Hair follicle dermal cells repopulate the mouse haematopoietic system. *J Cell Sci.* 2002; 115: 3967–74.
 51. **Richardson GD, Arnott EC, Whitehouse CJ, et al.** Plasticity of rodent and human hair follicle dermal cells: implications for cell therapy and tissue engineering. *J Invest Dermatol Symp Proc.* 2005; 10: 180–3.
 52. **Vaculik C, Schuster C, Bauer W, et al.** Human dermis harbors distinct mesenchymal stromal cell subsets. *J Invest Dermatol.* 2012; 132: 563–74.
 53. **Radu E, Simionescu O, Regalia T, et al.** Stem cells (p63(+)) in keratinocyte cultures from human adult skin. *J Cell Mol Med.* 2002; 6: 593–8.
 54. **Moore KA, Lemischka IR.** Stem cells and their niches. *Science.* 2006; 311: 1880–5.
 55. **Pasolli HA.** The hair follicle bulge: a niche for adult stem cells. *Microscop Microanal.* 2011; 17: 513–9.
 56. **Cotsarelis G.** Epithelial stem cells: a follicle-centric view. *J Invest Dermatol.* 2006; 126: 1459–68.
 57. **Li L, Mignone J, Yang M, et al.** Nestin expression in hair follicle sheath progenitor cells. *Proc Natl Acad Sci USA.* 2003; 100: 9958–61.
 58. **Sun TT, Cotsarelis G, Lavker RM.** Hair follicular stem cells: the bulge-activation hypothesis. *J Invest Dermatol.* 1991; 96: 77S–8S.
 59. **Kruse C, Bodo E, Petschnik AE, et al.** Towards the development of a pragmatic technique for isolating and differentiating nestin-positive cells from human scalp skin into neuronal and glial cell populations: generating neurons from human skin? *Exp Dermatol.* 2006; 15: 794–800.
 60. **Fuchs E.** Scratching the surface of skin development. *Nature.* 2007; 445: 834–42.
 61. **Ghazizadeh S, Taichman LB.** Multiple classes of stem cells in cutaneous epithelium: a lineage analysis of adult mouse skin. *EMBO J.* 2001; 20: 1215–22.